Pharmaceutical Sciences. 2025;31(3):294-303
doi:10.34172/PS.025.40914
https://ps.tbzmed.ac.ir/

Research Article

Phytosterol Glycosides from *Olax subscorpioidea* Oliv. Exhibit Cytotoxic Effects in *In Vitro* and *In Silico* Studies

Yemi A. Adekunle[1,2,3*], Babatunde B. Samuel[1], Lutfun Nahar[4*], Amos A. Fatokun[2], Satyajit D. Sarker[2]

[1]Department of Pharmaceutical Chemistry, Faculty of Pharmacy, University of Ibadan, Nigeria
[2]Centre for Natural Products Discovery, School of Pharmacy and Biomolecular Sciences, Faculty of Science, Liverpool John Moores University, Byrom Street, Liverpool L3 3AF, United Kingdom
[3]Department of Pharmaceutical and Medicinal Chemistry, College of Pharmacy, Afe Babalola University, Ado-Ekiti, Nigeria
[4]Laboratory of Growth Regulators, Palacký University and Institute of Experimental Botany, The Czech Academy of Sciences, Šlechtitelů 27, 78371 Olomouc, Czech Republic

ARTICLE INFO

Article History:
Received: December 10, 2024
Revised: March 4, 2025
Accepted: April 27, 2025
ePublished: June 17, 2025

Keywords:
Olax subscorpioidea, Cancer, NMR, Molecular docking, Stigmast-5,22-dien-3-O-*β*-D-glucoside, Sitosterol-3-O-*β*-D-glucoside

Abstract

Background: *Olax subscorpioidea* is traditionally used to treat arthritis, cancer, diabetes, neurodegenerative disorders, and oxidative stress. This study carried out chromatographic isolation, cytotoxicity, and molecular docking studies of bioactive compounds from *O. subscorpioidea*.

Methods: The root of *O. subscorpioidea* was extracted with methanol using the Soxhlet extraction method. The extract was partitioned into *n*-hexane, dichloromethane (DCM), and methanol/water. The DCM fraction was subjected to column chromatography. Bioactive compounds were isolated and their chemical structures were established by one-dimensional (1D) and two-dimensional (2D) nuclear magnetic resonance (NMR) spectroscopy, and by comparing their NMR data with those previously reported in the literature. 3-(4,5-dimethylthiazol-2-yl)-2,5-diphenyl-2H-tetrazolium bromide (MTT) assay was used to evaluate the cytotoxic activity of these compounds against three human cancer cell lines: breast (MCF-7), cervical (HeLa), and colorectal (Caco-2) cell lines. Molecular docking was used to gain insights into the favourable binding conformations and energies of the compounds when interacting with ten selected cancer-related protein targets.

Results: The phytochemical investigation of the extract of *O. subscorpioidea* afforded two sterol glycosides, stigmast-5,22-dien-3-*O*-*β*-D-glucoside (1a) and sitosterol-3-*O*-*β*-D-glucoside (1b), as a mixture. The compounds were found to be active against HeLa (IC_{50}: 37.0 ± 4.51 µg/mL) and MCF-7 (137.07 ± 19.43 µg/mL) cell lines. The compounds showed strong interactions with the colchicine-binding site on the *β*-subunit of tubulin protein, epidermal growth factor receptor kinase domain, poly(ADP-ribose) polymerase-1, and 17*β*-hydroxysteroid dehydrogenase type 1 (binding energies: –10.3 and –10.0 kcal/mol; –9.3 and –9.3 kcal/mol; –9.2 and –9.2 kcal/mol; and –9.3 and –9.1 kcal/mol, respectively). Stigmast-5,22-dien-3-*O*-*β*-D-glucoside was consistently ranked higher in some of the proteins tested. The compounds stabilised in the binding sites of the proteins via hydrogen bonds and hydrophobic interactions.

Conclusion: To the best of our knowledge, this is the first report on the isolation of these compounds from this plant. The cytotoxic effects of *O. subscorpioidea* root extract could be partly attributed to stigmast-5,22-dien-3-*O*-*β*-D-glucoside and sitosterol-3-*O*-*β*-D-glucoside.

Introduction

Plants have provided medicine for humans for many centuries.[1,2] A large percentage of the world's population, especially in developing countries, depend on medicinal plants as sources of medicines.[3] Secondary metabolites have been recognised as the healing principles in plants. Cancer is a leading cause of death globally.[4] It kills about 10 million people every year across the globe.[5] Approximately 70% of cancer-related deaths occur in low- and middle-income countries.[6] Many cancer drugs have been developed, the majority of which have serious adverse effects.[1,7] Therefore, there is a need for anticancer drugs that are more tolerable, effective, and less toxic.

Olax subscorpioidea Oliv. belongs to the Olacaceae family that comprises shrubs, trees and woody dicotyledonous plants with significant economic and medicinal values. This family includes a range of secondary metabolites, such as flavonoids, triterpenoids, and secoiridoids, each exhibiting diverse biological activities.[8-10] The plants, distributed within about 25 genera, are widely distributed in temperate and tropical regions.[9]

Olax subscorpioidea is a shrub-like tree that reaches

***Corresponding Authors:** Yemi A. Adekunle, Emails: y.a.adekunle@2022.ljmu.ac.uk; adekunleya@abuad.edu.ng and Lutfun Nahar, Email: profnahar@outlook.com

a height of approximately 10 metres.[11] The plant is traditionally used to treat arthritis, cancer, depression, diabetes mellitus, neurodegenerative disorders, oxidative stress, and swelling.[12,13] Ethnobotanical surveys showed that *O. subscorpioidea* is an important ingredient in traditional cancer remedies in Nigeria.[14-16] We recently reported cytotoxic triterpenoid saponins from *O. subscorpioidea*.[17]

The preliminary cytotoxic analysis of the methanol root extract of *O. subscorpioidea* showed antiproliferative activity against human rhabdomyosarcoma (RD) and breast cancer (MCF-7) cell lines.[18] The current study, therefore, aimed at isolating and characterising bioactive compounds from *O. subscorpioidea* root extract. The potential of these compounds as inhibitors of the growth of human cancer cell lines was evaluated by the MTT assay. Molecular docking and ADMET (absorption, distribution, metabolism, excretion, toxicity) studies were also conducted.

Methods

General experimental procedures

The infrared spectroscopy (IR) spectrum was obtained using a Cary 630 FTIR spectrophotometer (Agilent Technologies, USA). 1D and 2D nuclear magnetic resonance (NMR) data were obtained on a Bruker Avance III NMR spectrometer at 600 MHz (Bruker, USA). The sample was dissolved in dimethyl sulfoxide (DMSO-d6) and the solvent residue served as the internal standard. Chemical shifts (δ) were measured in parts per million (ppm), and coupling constants were measured in *hertz* (Hz). High-performance liquid chromatography (HPLC) grade solvents from Fisher Scientific (Loughborough, United Kingdom) were used. Cell culture materials include Dulbecco's Modified Eagle Medium (DMEM) (Thermo Fisher Scientific, UK), L-glutamine 200 mM (100X) (Gibco, UK), antibiotic-antimycotic (100X) (Gibco, UK), TrypLE Express (1X) (Thermo Fisher Scientific, UK), Fetal bovine serum (Sigma-Aldrich, UK), Phosphate buffered-saline (Thermo Fisher Scientific, UK), and MTT (Sigma-Aldrich, UK). Vinblastine from Tocris (UK) was used as a reference drug. Absorbance measurements were performed on a Tecan Spark 10M multimode microplate reader (Switzerland).

Plant collection

The root of *O. subscorpioidea* was collected in April 2021 from the University of Ibadan botanical garden, Ibadan, Nigeria. The collection and identification of the plant were performed by the garden curator, Mr Michael Owolabi. A sample was deposited at the Forest Herbarium, Ibadan (FHI) with voucher number FHI:113182. The root material was cleaned, peeled, and dried in the lab. After that, it was ground into powder.

Extraction and fractionation

Approximately 600 g of powdered *O. subscorpioidea* root material was extracted with methanol using the Soxhlet extraction method. The extract was concentrated *in vacuo* using a rotary evaporator at a temperature below 40 °C (Heidolph HB Digital, Germany). The resulting extract was dried at room temperature in the laboratory and stored for later use. About 63.7 g of extract was obtained. The extract was further partitioned into *n*-hexane, dichloromethane (DCM), and water/methanol. Approximately 40 g of the extract was dissolved in water/methanol (20/80%) in a separating funnel and partitioned with an equal volume of *n*-hexane. The hexane fraction was obtained and concentrated. The extraction was done three times. Into the aqueous fraction, an equal volume of DCM was added (extraction was carried out three times) and the fraction was concentrated. The aqueous fraction was also obtained and concentrated.

Isolation of bioactive compounds

The isolation of compounds was carried out on an open glass chromatographic column packed with 60-120 mesh silica gel. The DCM fraction, 5.48 g, was re-suspended and loaded on the chromatography column (75 cm × 3.5 cm). The sample was eluted with *n*-hexane/ethyl acetate 70%:30% to 100% ethyl acetate, followed by ethyl acetate/methanol, 90%:10%; 80%:20%; 70%:30%; 50%:50%; 30%:70%; and 0%:100%. A total of 64 fractions were obtained (approximately, 30 mL each), which were pooled into 5 (F1–F5) according to their retention factor (R*f*) pattern (F_{254} silica gel 60 TLC plate, 70/20/10% *n*-hexane/ethyl acetate/methanol). Fraction F4 was further purified by crystallisation to obtain a white amorphous powder. The substance contained a mixture of two compounds assigned as **1** (9.8 mg). The compound showed a retention factor (R*f*) of 0.6 in ethyl acetate/methanol 9.5/0.5%. Compound **1** was visualised under an ultraviolet (UV) lamp (UVITEC, Cambridge). The developed TLC plate (Figure S1) was detected by being sprayed with conc. H_2SO_4, and then left in the oven at 110°C for about 10 min (Oven DHG-9053A, Ocean Med, England).

Cytotoxic analysis

Cells and cell culture

Human Caco-2, HeLa, and MCF-7 cancer cell lines were originally obtained from the American Type Culture Collection (ATCC) or the European Collection of Authenticated Cell Cultures (ECACC). As previously described,[17] the cells were cultured in DMEM supplemented with 10% Foetal Bovine Serum (FBS), 1% 2 mM L-glutamine, and 1% penicillin-streptomycin-amphotericin B solution. They were maintained in a 37 °C incubator with a 5% CO_2 humidified atmosphere. Cells were passaged approximately twice weekly. Before the treatment, cells were seeded into 96-well microplates and incubated for 24 hours. Cell visualization (at × 10 magnification) was performed using an Olympus CKX41 inverted microscope.

Cell treatments and cell viability assessment with the MTT assay

Stock solutions were prepared in DMSO, and all further dilutions were made in full growth medium. The highest concentrations used contained no more than 0.1% DMSO, which was non-toxic to the cells. Each well containing approximately 7,500 cells, prepared as previously reported,[17] was treated with the sample (concentrations: 1, 10, 50, 100, and 200 µg/mL). Each experiment was performed in triplicate and repeated three independent times (n = 3). The effects on the viability of the three human cell lines of the isolated compounds were assessed using the *in vitro* MTT assay.[19]

Molecular docking study

Ligand, protein retrieval and preparation

The ligands used in this study were the structures of stigmast-5,22-dien-3-O-*β*-D-glucoside and sitosterol-3-*O*-*β*-D-glucoside isolated from the methanol root extract of *O. subscorpioidea*. Their structures were downloaded from the PubChem database (https://pubchem.ncbi.nlm.nih.gov/). The 3D structures were prepared for docking using the UCSF Chimera tool (1.16).[20] Gasteiger charges and hydrogen atoms were added.[21] Energy minimisation of the structures was carried out at 100 steepest descent steps.

The 3D structures of the following proteins were retrieved from the Protein Data Bank (PDB) (https://www.rcsb.org/).[22] Alpha-beta tubulin complexed with taxol (PDB ID: 1JFF),[23] alpha-beta tubulin complexed with colchicine (PDB ID: 1SA0),[24] caspase-3 (PDB ID: 1GFW),[25] human 17 beta-hydroxysteroid dehydrogenase-1 (PDB ID: 1FDW),[26] phosphoinositide 3-kinase (PDB ID: 1E8Z),[27] poly (ADP-ribose) polymerase-1 (PDB ID: 5DS3),[28] bromodomain-containing protein 4 (PDB ID: 7JKW),[29] epidermal growth factor receptor tyrosine kinase domain (PDB ID: 1M17),[30] human oestrogen receptor alpha (PDB ID: 3ERT),[31] and polo-like kinase-1 (PDB ID: 3FC2).[32] To prepare the proteins, they were individually uploaded to the workspace of Chimera. All ligands, small molecules, water, and other co-crystallised compounds were deleted. Hydrogen atoms were added to the proteins. In addition, partial charges were added by ANTECHAMBER. The structures were then minimised to 200 steepest descent steps at 10-minute intervals. The prepared proteins were saved in .pdb to be used for docking.[33]

Docking

A molecular docking study was carried out to obtain information about the various binding conformations and binding energies of the compounds when interacting with the selected proteins. A site-directed docking was performed for all proteins. First, they were uploaded to the GPU of the Python Prescription Virtual Screening Tool (PyRx). They were then made into macromolecules. The active site of each protein had been pre-determined as the residues within 5 Å region of the co-crystallised ligand in Chimera. The ligands were imported to the GPU of PyRx, converted to AutoDock ligand format (.pdbqt), and the grid box set, fitting the active site which was defined by the grid box coordinates as shown in Table 1. Docking was carried out with the AutoDock Vina of PyRx.[34] BIOVIA Discovery Studio Visualiser was used to analyse the protein-ligand interactions.[21]

ADMET study

Drug-likeness means how much a compound's properties resemble those of existing drugs. The physicochemical parameters and ADME properties of the isolated compounds were evaluated using a freely available web tool, SwissADME (http://www.swissadme.ch/).[35] Some of the parameters obtained include molecular weight, lipophilicity, hydrogen bond acceptors and donors, topological polar surface area (TPSA), enzyme inhibition, and synthetic route accessibility.

Statistical analysis

Each experiment was carried out three independent times (n = 3). Data is presented as mean of IC_{50} ± SEM (standard error of the mean). GraphPad Prism (9.4) was used to calculate the IC_{50}. One-way ANOVA was used to determine the statistical significance of differences between means ($P < 0.05$ considered significant).

Results and Discussion

Cytotoxic effects of O. subscorpioidea fractions

Olax subscorpioidea is found in many countries across West and Central Africa and its traditional applications include its use to treat cancer, diabetes mellitus, neurodegenerative disorders, and swelling.[12,13] An ethnobotanical study among people in Ogun State, Nigeria, discovered that a mixture containing *O. subscorpioidea* root, along with other plants including *Alafia barteri* leaf, *Anthocleista djalonensis* root, *Calliandra portoricensis* root, *Clausena anisata* stem bark, *Macaranga barteri* stem bark, *Tephrosia vogelii* stem bark, *Triclisia subcordata* leaf, *Xylopia aethiopica*, and potash, is used to treat breast cancer.[15] A preliminary study of the cytotoxic activity of *O. subscorpioidea* revealed activity against MCF-7 and RD.[18] The methanol root extract was further fractionated into *n*-hexane, DCM, and aqueous media. The DCM fraction showed the highest activity against the two cell lines with percentage cell inhibition of 80.08% for MCF-7 and 82.01% for RD. The activity was closely followed by that of the *n*-hexane fraction with percentage cell inhibition of 78.42% for MCF-7 and 79.98% for RD. The aqueous fraction showed lower activity, having cell inhibition of 8.46% for MCF-7 and 40.87% for RD.[18] The current study focused on isolating bioactive compounds from the DCM fraction and evaluating their cytotoxic effects against human cancer cell lines.

Structure determination

The DCM fraction yielded a white amorphous powder,

Table 1. Binding site coordinates of some protein targets

Dimensions	17*β*HDS1 (PDB ID: 1FDW)	PARP-1 (PDB ID: 5DS3)	EGFR (PDB ID: 1M17)	*αβ*-TUBULIN (PDB ID:1SA0)
Centre_x (Å)	46.2939	– 1.9486	24.6136	117.8476
Centre_y (Å)	7.0436	37.6889	–0.3664	89.7445
Centre_z (Å)	42.6282	13.7477	25.3674	6.5756
Size_x (Å)	23.8829	23.1186	28.0573	19.6719
Size_y (Å)	20.8675	18.1855	18.3221	25.6549
Size_z (Å)	22.8567	26.5048	21.7736	20.9588

9.8 mg (Compound **1**). Extensive NMR experiments revealed that the isolated compound was a mixture of two known sterol glycosides. In the ^{13}C NMR experiment, the signals at δ_C 101.05 and 101.27, and 121.66 and 121.69 occurred as pairs each indicating a mixture of two similar compounds. The heteronuclear multiple bond correlation (HMBC) spectrum was used to verify the identity of the individual compounds in each mixture, which were identified as stigmasterol glucoside and *β*-sitosterol glucoside by detecting the distinct signals at positions C-22 and C-23.[36] Using HMBC spectrum, the chemical shifts of stigmasterol glucoside at positions C-22 and C-23 were confirmed as 138.5 and 129.3 ppm, respectively, indicating the presence of an alkene group. In contrast, *β*-sitosterol glucoside showed chemical shift signals for C-22 and C-23 resonating at 33.8 and 25.9 ppm, respectively, suggesting an alkyl group (Table S1). Homonuclear correlation spectroscopy (^{1}H-^{1}H COSY), heteronuclear single quantum correlation (HSQC), and HMBC spectra helped confirm all ^{1}H and ^{13}C assignments (Figures 1a and 1b, and Figures S2–S7).

Stigmast-5,22-dien-3-*O*-*β*-D-glucoside (**1a**), white amorphous powder. IR: 3360 cm^{-1}, broad (OH stretch), 2910 cm^{-1} (CH stretch), and 1010 cm^{-1} (CO stretch). ^{1}H NMR (DMSO, 600 MHz): δ_H 2.12, 2.35 (2H, C-1), 3.45 (*m*, 1H, C-3), 1.79 (2H, C-4), 5.33 (*t*, 1H, C-6), 1.91 (2H, C-7), 1.43 (1H, C-8), 0.99 *m* (1H, C-14), 1.79 (2H, C-16), 0.66 (*s*, 3H, C-18), 0.95 (*s*, 3H, C-19), 0.99 (*d* 6.48 Hz, 3H, C-21), 5.15 (*m*, 1H, C-22), 5.02 (*m*, 1H, C-23), 1.50 (1H, C-24), 1.34 (1H, C-25), 0.82 (3H, C-26), 0.78 (*d* 2.32 Hz, 3H, C-27), 0.77 (3H, C-29), 4.20 (*d*, 7.84 Hz, C-1'). ^{13}C-DEPT-Q δ_C: 38.8 (C-1), 77.4 (C-3), 37.3 (C-4), 140.9 (C-5), 121.7 (C-6), 31.8 (C-7), 55.8 (C-17), 12.3 (C-18), 19.6 (C-19), 21.6 (C-21), 138.5 (C-22), 129.3 (C-23), 51.1 (C-24), 31.9 (C-25), 21.4 (C-26), 19.3 (C-27), 12.6 (C-29), 101.2 (C-1') 73.9 (C-2'), 77.2 (C-3'), 70.5 (C-4'), 77.2 (C-5'), 61.5 (C-6').[37-40]

Sitosterol-3-*O*-*β*-D-glucoside (**1b**), white amorphous powder. IR: 3360 cm^{-1}, broad (OH stretch), 2910 cm^{-1} (CH stretch), and 1010 cm^{-1} (CO stretch). ^{1}H NMR (DMSO, 600 MHz): δ_H 3.45 *m* (1H, C-3), 5.33 (*t*, 1H, C-6), 1.91 (2H, C-7), 0.99 *m* (1H, C-14), 1.38 (2H, C-15), 1.78 (2H, C-16), 1.13 (1H, C-17), 0.66 (*s*, 3H, C-18), 0.80 (*s*, 3H, C-19), 1.33 (1H, C-20), 0.95 (3H, C-21), 1.00, 1.29 (2H, C-22), 1.14 (2H, C-23), 0.91 (1H, C-24), 0.90 (*d*, 6.22 *Hz* C-27), 0.81 (3H, C-29), 4.20 (*d*, 7.84 *Hz* C-1'), 3.08 (1H, C-3'), 3.04 (1H, C-5'), 3.39, 3.63 (1H, C-6'). ^{13}C-DEP-Q δ_C: 36.7 (C-1), 29.0 (C-2), 77.3 (C-3), 140.9 (C-5), 121.7 (C-6), 50.1 (C-9), 36.7 (C-10), 21.1 (C-11), 37.3 (C-12), 56.6 (C-14), 25.4 (C-15), 28.3 (C-16), 55.9 (C-17), 12.2 (C-18), 20.2 (C-19), 36.0 (C-20), 19.4 (C-21), 33.8 (C-22), 25.9 (C-23), 45.6 (C-24), 29.2 (C-25), 19.4 (C-26), 19.1 (C-27), 23.1 (C-28), 12.3 (C-29), 101.1 (C-1'), 73.9 (C-2'), 77.2 (C-3'), 70.5 (C-4'), 77.2 (C-5'), 61.5 (C-6').[38,41,42]

The occurrence of *β*-sitosterol and stigmasterol or their glycosides together in the same plant is common. Similarly, the isolation of the two compounds or their glycosides together as a mixture is also frequent. Kamal et al[36] isolated a mixture of *β*-sitosterol and stigmasterol from *Vitex pinnata* L. Ekhuemelo et al[43] isolated a mixture of sitosterol, stigmasterol and cycloeucalenol from *Erythrophleum suaveolens* (Guill. & Perr.) Brenan. Here are a few other plants from which a mixture of the compounds was reported: *Baccaurea macrocarpa* Miq. Mull. Arg,[44] *Cassia sieberiana* DC.,[45] *Premna herbacea* Roxb.,[46] and *Ricinus communis* L.[47] Elfita et al[48] isolated a mixture of their glycosides from *Garcinia griffithii* T. Anderson. These compounds also exhibit a variety of biological activities.

Cytotoxic effects of the isolated compounds

The cytotoxic potencies of the isolated compounds, as indicated by the IC_{50} values, are presented in Table 2. Compound **1**, a mixture of stigmast-5,22-dien-3-*O*-*β*-D-glucoside (**1a**) and sitosterol-3-*O*-*β*-D-glucoside (**1b**), showed cytotoxicity against the HeLa and MCF-7 cell lines. Its most potent cytotoxicity was against the HeLa cell line, with an IC_{50} value of 37.0 ± 4.51 µM, although it also exhibited mild cytotoxicity against the MCF-7 cell line, with an IC_{50} value of 137.07 ± 19.43 µg/mL (Table 2). Ikpefan et al[49] reported that stigmast-5,22-dien-3-*O*-*β*-D-glucoside was sensitive to MCF-7 and NCI-H460 cell lines with GI_{50} values of 40.83 ± 0.1 and 58.83 ± 11.2 µM, respectively, using the sulforhodamine B (SRB) cytotoxicity assay. Quradha et al[42] reported that sitosterol-3-*O*-*β*-D-glucoside had moderate activity against the HeLa cell line, with a cell inhibition of 48%, and a weak effect on the 3T3 cell line (mouse fibroblast), with a cell inhibition of 39%. This compound isolated from the aerial part of *Cynara cardunculus* var. *altilis* was also shown to have an IC_{50} value of 53.6 µg/mL against the hepatocellular carcinoma (HepG2) cell line.[50] A study investigating the effects of sitosterol-3-*O*-*β*-D-glucoside on HepG2 and SMMC-7721 cells, via the Wnt/β-catenin

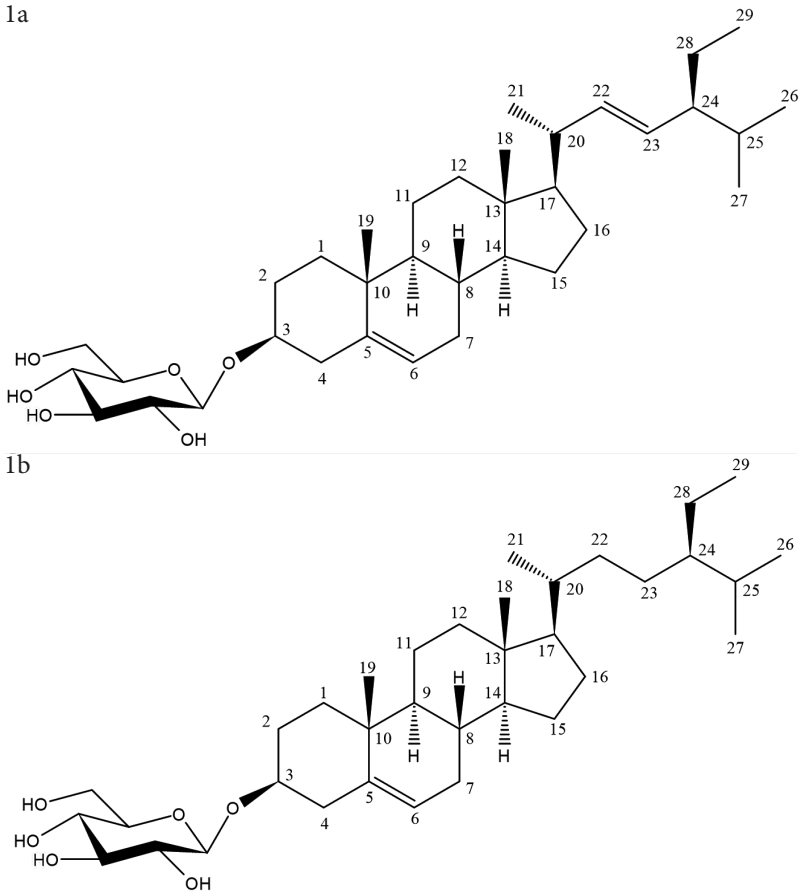

Figure 1. Structure of compound **1a** and **1b**

Table 2. Cytotoxic potencies (IC_{50}) of compounds **1a** and **1b** from *O. subscorpioidea* against human cancer cell lines

	IC_{50} ± SEM (µg/mL)		
Compounds	**HeLa**	**MCF-7**	**Caco-2**
1	37.0 ± 4.51	137.07 ± 19.43	>200
Vincristine	1.42 ± 0.40*	0.54 ± 0.06*	1.33 ± 0.05*

* Activities expressed in µM.

signalling pathway, found that it inhibited cell migration and invasion in HepG2 cells through this signalling pathway.[51] Another study revealed that sitosterol-3-*O*-*β*-D-glucoside exhibited its cytotoxic effects through the induction of apoptosis and activation of caspase-3 and -9 in the hepatocellular (Huh7 and HepG2) cancer cell lines.[52]

Molecular docking study

Molecular docking is a crucial computational tool in predicting binding conformations and binding energies of small molecule drugs (ligands) to receptor proteins, which enables high-throughput virtual screening.[53] In this study, ten cancer-related proteins were selected for the docking study. The compounds docked well with all the proteins. Stigmast-5,22-dien-3-*O*-*β*-D-glucoside consistently showed stronger interactions than sitosterol-3-*O*-*β*-D-glucoside with some of the proteins. The best interactions, with the least negative binding energies, were observed with alpha-beta tubulin complexed with colchicine (PDB ID: 1SA0). Compounds **1a** and **1b** showed binding energy of –10.3 and –10.0 kcal/mol, respectively. For compound **1a**, this was followed by epidermal growth factor receptor tyrosine kinase domain (EGFR) (PDB ID: 1M17) and 17β-hydroxysteroid dehydrogenase-1 (17β-HSD1) (PDB ID: 1FDW) with a binding energy of –9.3 kcal/mol. Poly (ADP-ribose) polymerase-1 (PARP-1) (PDB ID: 5DS3) had a binding energy of –9.2 kcal/mol for compound **1a**. For compound **1b**, EGFR ranked second with a binding energy of –9.3 kcal/mol, while PARP-1 had a binding energy of –9.2 kcal/mol (Table 3). The two compounds showed the least binding interactions with bromodomain-containing protein 4 (BRD4) (PDB ID: 7JKW) and caspase-3 (PDB ID: 1GFW).

The compounds show similar conformations at the colchicine-binding site of alpha-beta tubulin (Figures 2A and 3E). *αβ*-Tubulin heterodimers are microtubule proteins that are crucial for the mitotic phase of cell division. Classical inhibitors of the *β*-tubulin subunit act by promoting or disrupting microtubule assemblage during mitosis by binding to the colchicine-, vinca-, or taxol-binding sites.[54] The isolated compounds form a bridge between the *α*- and *β*-subunits of tubulin. The compounds were orientated in such a way that the

Table 3. Binding affinities of isolated compounds against ten selected protein targets

Ligands	PubChem ID	Binding affinities (kcal/mol)									
		1JFF	1GFW	1FDW	1E8Z	5DS3	7JKW	1M17	1SA0	3ERT	3FC2
1a	6602508	–9.0	–7.8	–9.3	–8.3	–9.2	–7.7	–9.3	–10.3	–8.2	–8.8
1b	12309057	–7.9	–7.7	–9.1	–7.7	–9.2	–7.4	–9.3	–10.0	–8.0	–8.8

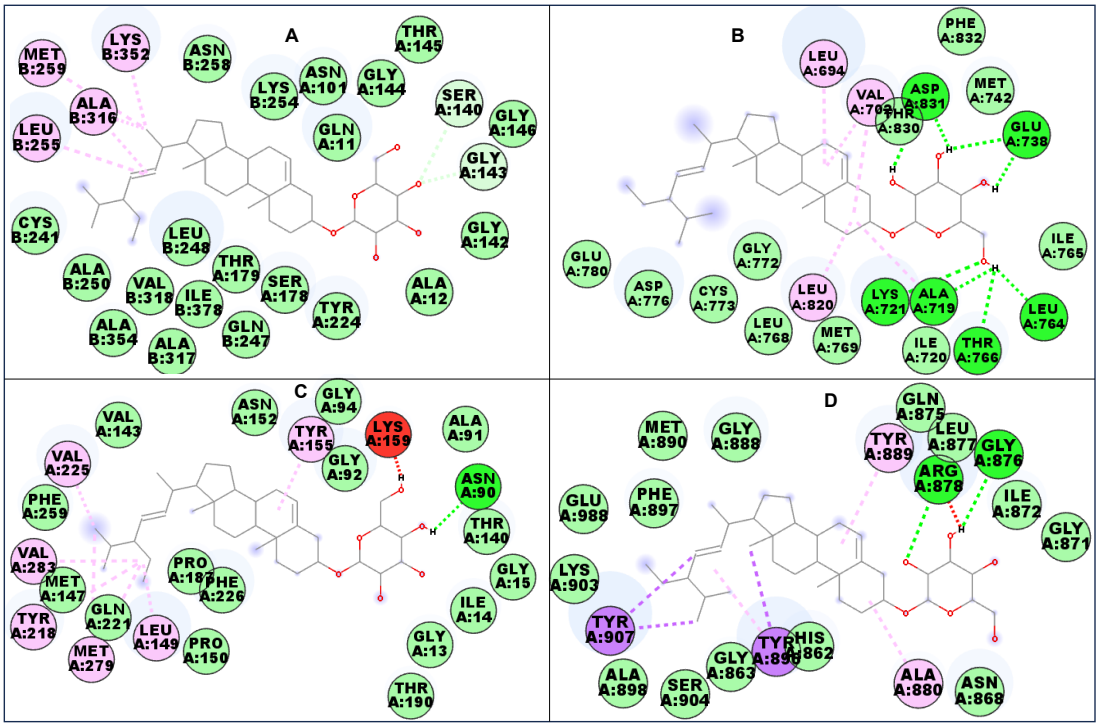

Figure 2. Interacting residues of (A) Alpha-beta tubulin, (B) EGFR, (C) 17β-HSD1, and (D) PARP-1 with compound 1a. Green: Conventional hydrogen bonding. Lilac: Alkyl/pi-alkyl interaction. Blue: Carbon hydrogen bonding. Purple: Pi-sigma bonding. Light green: van der Waals forces

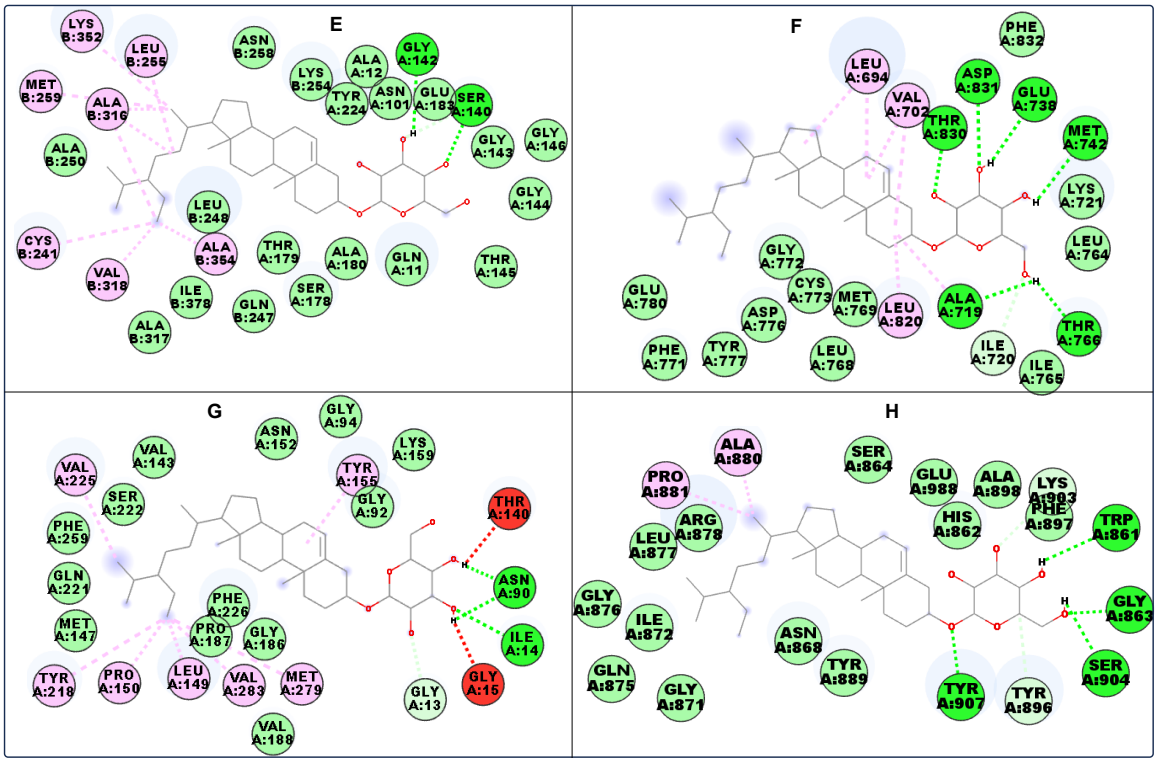

Figure 3. Interacting residues of (E) Alpha-beta tubulin, (F) EGFR, (G) 17β-HSD1, and (H) PARP-1 with compound 1b. Green: Conventional hydrogen bonding. Lilac: Alkyl/pi-alkyl interaction. Blue: Carbon hydrogen bonding. Purple: Pi-sigma bonding. Light green: van der Waals forces

polar glycosidic tail pointed toward the α-chain, while the non-polar head formed hydrophobic interactions with the β-chain. The compounds were observed to stabilise at the colchicine-binding pocket with crucial amino acid residues such as threonine (THR) 179 and cysteine (CYS) 241, the residues that have been implicated in the binding of colchicine-like compounds to the protein.[54] Similarly, colchicine hydrogen bonds with the CYS241 residue of β-tubulin and shows hydrophobic interaction.[55]

17β-HSD1 converts weakly active oestrone to a pharmacologically more active estrogen, 17β-oestradiol, in the breast tissue using nicotinamide adenine dinucleotide (NADH) or its phosphate (NADPH) as a cofactor. 17β-oestradiol is crucial for the growth of breast cancer cells.[56] The two compounds interacted with important 17β-HSD1 residues involved in its catalytic functions, which include tyrosine (TYR) 155 and lysine (LYS) 159 (Figures 2C and 3G).[57] EGFR residues interacted with the compounds via alkyl, van der Waals, and hydrogen bonds (Figures 2B and 3F). The sugar moiety was used to interact with the protein via hydrogen bonding. In PARP-1, compound **1a** formed a π-sigma bond with the protein in addition to alkyl, π-alkyl, van der Waals, and hydrogen bondings (Figures 2D and 3H). Since most of the selected proteins are expressed in the tested cancer cell lines, it can be suggested that the *in silico* study supports the *in vitro* study.

Drug-likeness study

In 1997, Christopher Lipinski from Pfizer introduced the "Rule of 5." It suggests that orally administered drugs are less likely to be absorbed or permeate well if they have a molecular weight exceeding 500 g/mol, more than 5 hydrogen bond donors, more than 10 hydrogen bond acceptors, or a CLog *P* greater than 5.[58] Although the "Rule of Five" is not sacrosanct because many blockbuster drugs in the clinic fail it, it has greatly helped in lead optimisation and drug design. In drug development, a drug candidate is assessed for its absorption, distribution, metabolism and elimination.[35] Table 4 shows the physicochemical parameters and ADMET descriptors for the isolated compounds 1a and 1b as virtually estimated by the SwissADME software. The compounds have molecular weights greater than 500 g/mol, which violate the Rule of 5. However, other parameters (Log P, hydrogen bond acceptor and hydrogen bond donor) are within acceptable ranges. The compounds are also not inhibitors of metabolic enzymes.

Table 4. Physicochemical/ADME descriptors of the isolated compounds

Parameters	1a	1b
Molecular weight (g/mol)	574.83	576.85
Num. rotatable bonds	8	9
Num. H-bond acceptors	6	6
Num. H-bond donors	4	4
TPSA (Å²)	99.38	99.38
Log $P_{o/w}$	4.23	4.98
CYP1A2 inhibitor	No	No
CYP2C19 inhibitor	No	No
CYP2C9 inhibitor	No	No
CYP2D6 inhibitor	No	No
CYP3A4 inhibitor	No	No
Synthetic accessibility	7.93	8.02

The bioavailability radar helps in the initial evaluation of how drug-like a molecule is, using the following physicochemical properties: Lipophilicity (LIPO), Flexibility (FLEX), Insaturation (INSATU), Insolubility (INSOLU), Polarity (POLAR), and Size (SIZE) (Figure 4). Lipophilicity is measured by Log *P*, which ranges from −0.7 to + 5.0. Size is assessed by molecular weight (≤ 500 g/mol). Polarity is indicated by TPSA (≤ 140 Å²). Insolubility is represented by log *S*. Insaturation is evaluated based on the fraction of carbon atoms in sp^3 hybridization. Flexibility is measured by the number of rotatable bonds (≤ 9).[59] The bioavailability radar in Figure 4 shows that the bioavailability rating of the two compounds was slightly within the suitable physicochemical space for oral bioavailability (www.swissadme.ch).

Conclusion

Medicinal plants are a productive source of drugs, including anticancer agents. In this study, stigmast-5,22-dien-3-*O*-β-D-glucoside and sitosterol-3-*O*-β-D-glucoside were isolated from the methanol root extract of *O. subscorpioidea*. Their structures were established by various spectroscopic data analyses (FTIR (Figure S8), 1D & 2D NMR). The results of the MTT assay show that the compounds were cytotoxic against human cervical (HeLa) and breast (MCF-7) cancer cell lines, with IC_{50} values of 37.0 ± 4.51 and 137.07 ± 19.43 µg/mL, respectively. The results of the docking analysis of the isolated compounds showed they had strong binding affinities for the colchicine-binding site of alpha-beta tubulin, epidermal growth factor receptor kinase, poly (ADP-ribose) polymerse-1, and 17β-hydroxysteroid dehydrogenase-1. To the best of our knowledge, this is the first report of the isolation of these compounds from *O. subscorpioidea*. These isolated compounds may, therefore, contribute to the cytotoxic effects of *O. subscorpioidea.*

Acknowledgements

Yemi A. Adekunle acknowledges the award of a Commonwealth Split-Site PhD Scholarship by the Government of the United Kingdom to visit Liverpool John Moores University for part of his PhD research (NGCN-2021-184). Lutfun Nahar gratefully acknowledges the financial support of the European Regional Development Fund - Project ENOCH (No. CZ.02.1.01/0.0/0.0/16 _019/0000868) and the Czech Agency Grants - Project 23-05474S and Project 23-05389S.

Authors' Contribution

Conceptualization: Yemi A. Adekunle, Babatunde B. Samuel.
Formal analysis: Yemi A. Adekunle, Babatunde B. Samuel.
Funding acquisition: Yemi A. Adekunle, Lutfun Nahar.

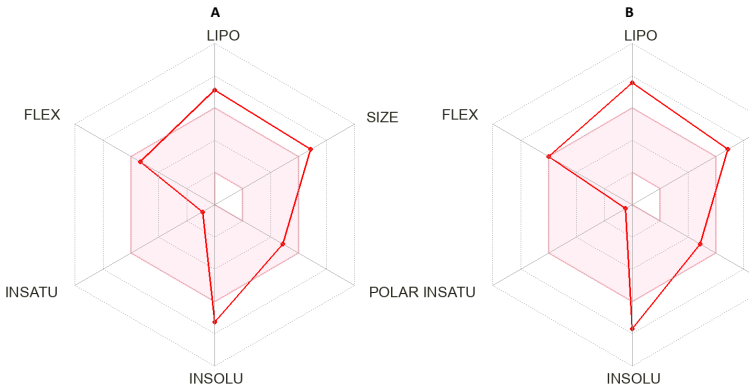

Figure 4. Bioavailability radar for the isolated compounds 1a (A) and 1b (B). LIPO: Lipophilicity. FLEX: Flexibility. INSATU: Insaturation. INSOLU: Insolubility. POLAR: Polarity. SIZE: Size

Formal analysis: Amos A. Fatokun.
Investigation: Yemi A. Adekunle.
Methodology: Yemi A. Adekunle.
Supervision: Babatunde B. Samuel, Lutfun Nahar, Satyajit D. Sarker.
Validation: Satyajit D. Sarker.
Writing–original draft: Yemi A. Adekunle.
Writing–review & editing: Lutfun Nahar, Amos A. Fatokun, Satyajit D. Sarker.

Competing Interests
The authors declare no conflicts of interests.

Ethical Approval
Not applicable.

Funding
This study was supported by the following grants: a Commonwealth Split-Site PhD Fellowship awarded to Yemi A. Adekunle (Ref.: NGCN-2021-184); the European Regional Development Fund—Project ENOCH (No. CZ.02.1.01/0.0/0.0/16_019/0000868); and Czech Agency Grants (Projects 23-05474S and 23-05389S) awarded to Lutfun Nahar.

Supplementary Files
Supplementary file 1 contains Table S1 and Figures S1-S8.

References
1. Sarker SD, Nahar L, Miron A, Guo M. Anticancer natural products. In: Sarker SD, Nahar L, eds. Annual Reports in Medicinal Chemistry. Vol 55. Academic Press; 2020. p. 45-75. doi: 10.1016/bs.armc.2020.02.001.
2. Newman DJ, Cragg GM. Natural products as sources of new drugs over the nearly four decades from 01/1981 to 09/2019. J Nat Prod. 2020;83(3):770-803. doi: 10.1021/acs.jnatprod.9b01285.
3. Ahmad Khan MS, Ahmad I. Herbal medicine: current trends and future prospects. In: Ahmad Khan MS, Ahmad I, Chattopadhyay D, eds. New Look to Phytomedicine. Academic Press; 2019. p. 3-13. doi: 10.1016/b978-0-12-814619-4.00001-x.
4. Sung H, Ferlay J, Siegel RL, Laversanne M, Soerjomataram I, Jemal A, et al. Global cancer statistics 2020: GLOBOCAN estimates of incidence and mortality worldwide for 36 cancers in 185 countries. CA Cancer J Clin. 2021;71(3):209-49. doi: 10.3322/caac.21660.
5. Ferlay J, Colombet M, Soerjomataram I, Parkin DM, Piñeros M, Znaor A, et al. Cancer statistics for the year 2020: an overview. Int J Cancer. 2021;149(4):778-89. doi: 10.1002/ijc.33588.
6. Kuete V, Efferth T. African flora has the potential to fight multidrug resistance of cancer. Biomed Res Int. 2015;2015:914813. doi: 10.1155/2015/914813.
7. Gyanani V, Haley JC, Goswami R. Challenges of current anticancer treatment approaches with focus on liposomal drug delivery systems. Pharmaceuticals (Basel). 2021;14(9):835. doi: 10.3390/ph14090835.
8. Hashmi MA, Khan A, Hanif M, Farooq U, Perveen S. Traditional uses, phytochemistry, and pharmacology of *Olea europaea* (Olive). Evid Based Complement Alternat Med. 2015;2015:541591. doi: 10.1155/2015/541591.
9. Huang YL, Oppong MB, Guo Y, Wang LZ, Fang SM, Deng YR, et al. The Oleaceae family: a source of secoiridoids with multiple biological activities. Fitoterapia. 2019;136:104155. doi: 10.1016/j.fitote.2019.04.010.
10. Mansour KA, Elbermawi A, Al-Karmalawy AA, Lahloub MF, El-Neketi M. Cytotoxic effects of extracts obtained from plants of the Oleaceae family: bio-guided isolation and molecular docking of new secoiridoids from *Jasminum humile*. Pharm Biol. 2022;60(1):1374-83. doi: 10.1080/13880209.2022.2098346.
11. Odoma S, Umar Zezi A, Mohammed Danjuma N, Ahmed A, Garba Magaji M. Elucidation of the possible mechanism of analgesic actions of butanol leaf fraction of *Olax subscorpioidea* Oliv. J Ethnopharmacol. 2017;199:323-7. doi: 10.1016/j.jep.2016.12.052.
12. Agbabiaka TO, Adebayo IA. The medicinal properties of *Olax subscorpioidea*. In: Bhat RA, Hakeem KR, Dervash MA, eds. Phytomedicine. Academic Press; 2021. p. 555-80. doi: 10.1016/b978-0-12-824109-7.00019-4.
13. Adekunle Y, Samuel BB, Fatokun AA, Nahar L, Sarker SD. *Olax subscorpioidea* Oliv. (Olacaceae): an ethnomedicinal and pharmacological review. J Nat Prod Discov. 2022;1(2):673. doi: 10.24377/jnpd.article673.
14. Soladoye MO, Amusa NA, Raji-Esan SO, Chukwuma EC, Taiwo AA. Ethnobotanical survey of anti-cancer plants in Ogun state, Nigeria. Ann Biol Res. 2010;1(4):261-73.
15. Gbadamosi IT, Erinoso SM. A review of twenty ethnobotanicals used in the management of breast cancer in Abeokuta, Ogun state, Nigeria. Afr J Pharm Pharmacol. 2016;10(27):546-64. doi: 10.5897/ajpp2015.4327.
16. Segun PA, Ogbole OO, Ajaiyeoba EO. Medicinal plants used in the management of cancer among the Ijebus of southwestern Nigeria. J Herb Med. 2018;14:68-75. doi: 10.1016/j.hermed.2018.04.002.
17. Adekunle YA, Samuel BB, Nahar L, Fatokun AA, Sarker SD. Cytotoxic triterpenoid saponins from the root of *Olax subscorpioidea* Oliv. (Olacaceae). Phytochemistry. 2023;215:113853. doi: 10.1016/j.phytochem.2023.113853.
18. Adekunle Y, Samuel B, Emmanuel T, Adeniji J, Ogbole O.

Cytotoxicity analysis of nineteen medicinal plants extracts on breast adenocarcinoma (MCF-7) and rhabdomyosarcoma (RD) cancer cell lines. Trends Pharm Sci. 2022;8(1):57-64. doi: 10.30476/tips.2022.94313.1136.
19. Mosmann T. Rapid colorimetric assay for cellular growth and survival: application to proliferation and cytotoxicity assays. J Immunol Methods. 1983;65(1-2):55-63. doi: 10.1016/0022-1759(83)90303-4.
20. Pettersen EF, Goddard TD, Huang CC, Couch GS, Greenblatt DM, Meng EC, et al. UCSF Chimera--a visualization system for exploratory research and analysis. J Comput Chem. 2004;25(13):1605-12. doi: 10.1002/jcc.20084.
21. Adewumi AT, Oluyemi WM, Adekunle YA, Adewumi N, Alahmdi MI, Soliman ME, et al. Propitious indazole compounds as β-ketoacyl-ACP synthase inhibitors and mechanisms unfolded for TB cure: integrated rational design and MD simulations. ChemistrySelect. 2023;8(3):e202203877. doi: 10.1002/slct.202203877.
22. Berman HM, Westbrook J, Feng Z, Gilliland G, Bhat TN, Weissig H, et al. The protein data bank. Nucleic Acids Res. 2000;28(1):235-42. doi: 10.1093/nar/28.1.235.
23. Löwe J, Li H, Downing KH, Nogales E. Refined structure of alpha beta-tubulin at 3.5 Å resolution. J Mol Biol. 2001;313(5):1045-57. doi: 10.1006/jmbi.2001.5077.
24. Ravelli RB, Gigant B, Curmi PA, Jourdain I, Lachkar S, Sobel A, et al. Insight into tubulin regulation from a complex with colchicine and a stathmin-like domain. Nature. 2004;428(6979):198-202. doi: 10.1038/nature02393.
25. Lee D, Long SA, Adams JL, Chan G, Vaidya KS, Francis TA, et al. Potent and selective nonpeptide inhibitors of caspases 3 and 7 inhibit apoptosis and maintain cell functionality. J Biol Chem. 2000;275(21):16007-14. doi: 10.1074/jbc.275.21.16007.
26. Mazza C, Breton R, Housset D, Fontecilla-Camps JC. Unusual charge stabilization of NADP+in 17beta-hydroxysteroid dehydrogenase. J Biol Chem. 1998;273(14):8145-52. doi: 10.1074/jbc.273.14.8145.
27. Walker EH, Pacold ME, Perisic O, Stephens L, Hawkins PT, Wymann MP, et al. Structural determinants of phosphoinositide 3-kinase inhibition by wortmannin, LY294002, quercetin, myricetin, and staurosporine. Mol Cell. 2000;6(4):909-19. doi: 10.1016/s1097-2765(05)00089-4.
28. Dawicki-McKenna JM, Langelier MF, DeNizio JE, Riccio AA, Cao CD, Karch KR, et al. PARP-1 activation requires local unfolding of an autoinhibitory domain. Mol Cell. 2015;60(5):755-68. doi: 10.1016/j.molcel.2015.10.013.
29. Li Y, Zhao J, Gutgesell LM, Shen Z, Ratia K, Dye K, et al. Novel pyrrolopyridone bromodomain and extra-terminal motif (BET) inhibitors effective in endocrine-resistant ER+breast cancer with acquired resistance to fulvestrant and palbociclib. J Med Chem. 2020;63(13):7186-210. doi: 10.1021/acs.jmedchem.0c00456.
30. Stamos J, Sliwkowski MX, Eigenbrot C. Structure of the epidermal growth factor receptor kinase domain alone and in complex with a 4-anilinoquinazoline inhibitor. J Biol Chem. 2002;277(48):46265-72. doi: 10.1074/jbc.M207135200.
31. Shiau AK, Barstad D, Loria PM, Cheng L, Kushner PJ, Agard DA, et al. The structural basis of estrogen receptor/coactivator recognition and the antagonism of this interaction by tamoxifen. Cell. 1998;95(7):927-37. doi: 10.1016/s0092-8674(00)81717-1.
32. Rudolph D, Steegmaier M, Hoffmann M, Grauert M, Baum A, Quant J, et al. BI 6727, a polo-like kinase inhibitor with improved pharmacokinetic profile and broad antitumor activity. Clin Cancer Res. 2009;15(9):3094-102. doi: 10.1158/1078-0432.Ccr-08-2445.
33. Oluyemi WM, Samuel BB, Adewumi AT, Adekunle YA, Soliman MES, Krenn L. An allosteric inhibitory potential of triterpenes from *Combretum racemosum* on the structural and functional dynamics of *Plasmodium falciparum* lactate dehydrogenase binding landscape. Chem Biodivers. 2022;19(2):e202100646. doi: 10.1002/cbdv.202100646.
34. Trott O, Olson AJ. AutoDock Vina: improving the speed and accuracy of docking with a new scoring function, efficient optimization, and multithreading. J Comput Chem. 2010;31(2):455-61. doi: 10.1002/jcc.21334.
35. Daina A, Michielin O, Zoete V. SwissADME: a free web tool to evaluate pharmacokinetics, drug-likeness and medicinal chemistry friendliness of small molecules. Sci Rep. 2017;7:42717. doi: 10.1038/srep42717.
36. Kamal N, Clements C, Gray AI, Edrada-Ebel R. Anti-infective activities of secondary metabolites from *Vitex pinnata*. J Appl Pharm Sci. 2016;6(1):102-6. doi: 10.7324/japs.2016.600117.
37. Falodun A, Ali S, Quadir IM, Choudhary IM. Phytochemical and biological investigation of chloroform and ethylacetate fractions of *Euphorbia heterophylla* leaf (Euphorbiaceae). J Med Plants Res. 2008;2(12):365-9.
38. Khatun M, Billah M, Quader MA. Sterols and sterol glucoside from *Phyllanthus* species. Dhaka Univ J Sci. 2012;60(1):5-10. doi: 10.3329/dujs.v60i1.10327.
39. Ridhay A, Noor A, Soekamto NH, Harlim T, van Altena I. A stigmasterol glycoside from the root wood of *Melochia umbellata* (Houtt) Stapf var. degrabrata K. Indones J Chem. 2012;12(1):100-3. doi: 10.22146/ijc.21379.
40. Rosli N, Khairuddean M, Jamain Z. Phytochemical and biological activity studies of the leaves of *Garcinia hombroniana* Pierre. Malays J Chem. 2020;22(4):81-102.
41. Peshin T, Kar HK. Isolation and characterization of β-sitosterol-3-O-β-D-glucoside from the extract of the flowers of *Viola odorata*. Br J Pharm Res. 2017;16(4):1-8. doi: 10.9734/bjpr/2017/33160.
42. Quradha MM, Khan R, Adhikari A, Rauf A, Rashid U, Bawazeer S, et al. Isolation, biological evaluation, and molecular docking studies of compounds from *Sophora mollis* (Royle) Graham ex Baker. ACS Omega. 2021;6(24):15911-9. doi: 10.1021/acsomega.1c01532.
43. Ekhuemelo DO, Agbidye FS, Anyam JV, Ekhuemelo C, Igoli JO. Antibacterial activity of triterpenes from the stem bark and heartwood of *Erythrophleum suaveolens* (Guill. & Perr.) Brenan. J Appl Sci Environ Manag. 2019;23(5):783-9. doi: 10.4314/jasem.v23i5.2.
44. Erwin, Pusparohmana WR, Safitry RD, Marliana E, Usman, Kusuma IW. Isolation and characterization of stigmasterol and β-sitosterol from wood bark extract of *Baccaurea macrocarpa* Miq. Mull. Arg. Rasayan J Chem. 2020;13(4):2552-8. doi: 10.31788/rjc.2020.1345652.
45. Khan ME, Odokpe AU, Tor-Anyiin TA. Isolation and characterization of stigmasterol and β-sitosterol from *Cassia sieberiana* (Fabaceae) leaf extract. J Chem Soc Nigeria. 2020;45(1):135-42.
46. Shwe HH, Thein WW, Win SS, Pe NN, Win T. Structural characterization of stigmasterol and β-sitosterol from the roots of *Premna herbacea* Roxb. Int Eur Ext Enablement Sci Eng Manag. 2019;7(8):195-201.
47. Masoko P, Nemudzivhadi V. Isolation and chemical structural characterization of the mixture of two related phytosterols from *Ricinus communis* L. (Euphorbiaceae) leaves. European J Med Plants. 2015;10(2):1-11. doi: 10.9734/ejmp/2015/18172.
48. Elfita E, Muharni M, Latief M, Darwati D, Widiyantoro A, Supriyatna S, et al. Antiplasmodial and other constituents from four Indonesian *Garcinia* spp. Phytochemistry. 2009;70(7):907-12. doi: 10.1016/j.phytochem.2009.04.024.
49. Ikpefan EO, Ayinde BA, Omeje EO, Azhar M, Farooq AD, Shah ZA, et al. Isolation and anti-cancer evaluation of two anti-proliferative constituents from the chloroform fraction of leaves of *Conyza sumatrensis* (Retz.) E. H. Walker, Asteraceae. Sci Afr. 2021;13:e00854. doi: 10.1016/j.sciaf.2021.e00854.

50. Hamza RA, Mostafa I, Mohamed YS, Dora GA, Ateya AM, Abdelaal M, et al. Bioguided isolation of potential antitumor agents from the aerial parts of cultivated cardoon (*Cynara cardunculus* var. *altilis*). Saudi Pharm J. 2023;31(1):125-34. doi: 10.1016/j.jsps.2022.11.011.
51. Zeng J, Liu X, Li X, Zheng Y, Liu B, Xiao Y. Daucosterol inhibits the proliferation, migration, and invasion of hepatocellular carcinoma cells via Wnt/β-catenin signaling. Molecules. 2017;22(6):862. doi: 10.3390/molecules22060862.
52. Vo TK, Ta QTH, Chu QT, Nguyen TT, Vo VG. Anti-hepatocellular-cancer activity exerted by β-sitosterol and β-sitosterol-glucoside from *Indigofera zollingeriana* Miq. Molecules. 2020;25(13). doi: 10.3390/molecules25133021.
53. Hou X, Du J, Zhang J, Du L, Fang H, Li M. How to improve docking accuracy of AutoDock4.2: a case study using different electrostatic potentials. J Chem Inf Model. 2013;53(1):188-200. doi: 10.1021/ci300417y.
54. Horgan MJ, Zell L, Siewert B, Stuppner H, Schuster D, Temml V. Identification of novel β-tubulin inhibitors using a combined in silico/in vitro approach. J Chem Inf Model. 2023;63(20):6396-411. doi: 10.1021/acs.jcim.3c00939.
55. Naaz F, Haider MR, Shafi S, Yar MS. Anti-tubulin agents of natural origin: targeting taxol, vinca, and colchicine binding domains. Eur J Med Chem. 2019;171:310-31. doi: 10.1016/j.ejmech.2019.03.025.
56. Lawrence HR, Vicker N, Allan GM, Smith A, Mahon MF, Tutill HJ, et al. Novel and potent 17beta-hydroxysteroid dehydrogenase type 1 inhibitors. J Med Chem. 2005;48(8):2759-62. doi: 10.1021/jm049045r.
57. Frotscher M, Ziegler E, Marchais-Oberwinkler S, Kruchten P, Neugebauer A, Fetzer L, et al. Design, synthesis, and biological evaluation of (hydroxyphenyl)naphthalene and -quinoline derivatives: potent and selective nonsteroidal inhibitors of 17beta-hydroxysteroid dehydrogenase type 1 (17beta-HSD1) for the treatment of estrogen-dependent diseases. J Med Chem. 2008;51(7):2158-69. doi: 10.1021/jm701447v.
58. Lipinski CA. Drug-like properties and the causes of poor solubility and poor permeability. J Pharmacol Toxicol Methods. 2000;44(1):235-49. doi: 10.1016/s1056-8719(00)00107-6.
59. Rai M, Singh AV, Paudel N, Kanase A, Falletta E, Kerkar P, et al. Herbal concoction unveiled: a computational analysis of phytochemicals' pharmacokinetic and toxicological profiles using novel approach methodologies (NAMs). Curr Res Toxicol. 2023;5:100118. doi: 10.1016/j.crtox.2023.100118.